2003/05

INVESTIGATION AND SIMULATION OF THE THERMAL FATIGUE BEHAVIOUR OF A HOT WORKING TOOL STEEL EMPLOYING PULSED LASER RADIATION

I. Siller *,[a], W. Waldhauser [b], R. Ebner [a,b], T. Antretter[c]

The thermal fatigue behaviour of a hot working tool steel was investigated by employing pulsed laser radiation to generate surface near cyclic temperature fields. A special thermal fatigue testing facility was designed and built-up for performing the experiments. To prevent oxidation a disk shaped specimen was tested in a vacuum chamber using a pulsed 1.8 kW diode laser as heating source. Preheating of the specimen was applied to achieve temperature cycles similar to thermal cycles in manufacturing tools. Maximum surface temperatures of about 575, 600, 625 and 650 °C were applied in the experiments by varying the laser pulse energies. The experiments were done on a hot working tool steel DIN X 38 CrMoV 5 1 (Werkst.-Nr. 1.2343). The thermal fatigue behaviour of the material was characterised by the number of cycles to form a crack network and by investigating the hardness change of the irradiated surface. Finite element calculations were used to support the experimentation and to estimate the resulting cyclic strains and stresses.

1 INTRODUCTION

Thermal fatigue is an important damage mechanism, which significantly affects the lifetime of tools, e.g. dies, which are subjected to cyclic thermal loads. In processes like hot forging, casting, hot-rolling or extrusion, dies are not only subjected to mechanical loading, but also to thermo-mechanical loads induced by the repeated contact with the hot metal of the work piece [1]. Thermal stresses arise in case of inhomogeneous heating due to internal constraint. Cyclic thermal stresses can lead to fatigue damage.

Various measures can be taken to prevent thermally induced fatigue failure or to postpone it to higher numbers of cycles [2]: (1) The design of parts can be altered to

* Corresponding author

[a] Materials Center Leoben, Competence Center within the framework of the Kplus Programme, Leoben, Austria

[b] Laser Center Leoben, JOANNEUM RESEARCH Forschungsgesellschaft mbH, Leoben, Austria

[c] Institute for Mechanics, University of Leoben, Austria

Anhang 2

minimize the effect of oscillating stresses. (2) The materials resistance to fatigue failure can be increased.

In the case of manufacturing tools the maximum surface temperature, which is achieved in the manufacturing process strongly, depends on the process type and the parameters. E.g. for aluminium pressure die-casting the surface temperatures are in the range of about 500–650 °C [3]. Normally, the background temperature of dies is held constant at a temperature level of about 200-250 °C in order to reduce the thermal stresses.

Aim of the present work is to study the behaviour of a common tool steel under loading spectra which are comparable to that of manufacturing tools. Main emphasis was put on a combined theoretical and experimental treatment of the complex loading situation resulting from cyclic temperature fields. A special thermal fatigue testing system was developed and built-up in order to investigate the thermal fatigue behaviour experimentally. This testing system employs pulsed laser radiation for simulating the thermal fatigue behaviour physically in short time and under well-defined conditions. FEM simulations were carried out to design the test set-up and for the determination of the thermo-mechanical loading due to the pulsed laser beam radiation.

For characterising the thermal fatigue behaviour the irradiated material surface was inspected after defined numbers of cycles by means of scanning electron microscopy to search for changes in the surface morphology and to identify preferred crack nucleation sites. Additional hardness measurements were performed to get information about the changes of the material due to the irradiation.

2 EXPERIMENTAL

2.1. Material and test sample

All tests were performed at the hot work tool steel DIN X 38 CrMoV 5 1, its nominal chemical composition is shown in Table 1. The specimens were tested in a quenched and tempered condition (austenitizing: 990 °C - 50 min, tempering: 550 °C - 1h and 575 °C - 2 h) at a hardness level of 502 HV1.

Table 1 Nominal chemical compositions of the X 38 CrMoV 5 1 in wt.%

	C	Cr	W	Mo	V
X 38 CrMoV 5 1	0.38	5	-	2.8	0.65

The thermo-mechanical behaviour was characterised by tensile tests in the temperature range from room temperature to 650°C and strain rates ranging from 2.10^{-2} to 2 s^{-1}. Some results of the mechanical tests are shown in Table 2. The

hardness was determined by Vickers hardness testing at a load of 10 N. The fatigue tests were performed at ground and polished discs with a diameter of 22.5 mm and a thickness of 3.1 mm which were mechanically fixed to a temperature controlled specimen holder.

Table 2 Tensile properties of the investigated steel X 38 CrMoV 5 1 at strain rate of 0,02 s^{-1}.

Temperature [°C]	Yield Strength Rp 0,2 [MPa]	Tensile Strength Rm [MPa]
500	1015	1295
575	851	1114
650	431	598

2.2. Thermal fatigue testing facility and test conditions

A specially designed thermal fatigue testing facility was developed to study the thermal fatigue behaviour of tool steels, see Figure 1.

The disk shaped specimen is tested in a vacuum chamber to prevent oxidation of the heated surface. All tests were carried out under vacuum at a pressure lower than 3.10^{-6} mbar. No significant oxidation is observed even for the longest testing time of seven days. The sample is mechanically fixed on a temperature-controlled copper mounting system, which is held at a constant temperature of 200°C for all tests. Cyclic surface heating is done using a pulsed diode laser beam with a maximum power of about 1,8 kW. All tests are performed at a frequency of 1 Hertz and a pulse duration of 250 ms. Variations of the pulse energy are used to vary the maximum surface temperature. The laser radiation is guided via an optical fibre, a focussing unit and a transparent window to the specimen. A circular area with a diameter of about 6 mm is irradiated. The reflected laser radiation is absorbed in a water-cooled beam dump. The temperature in the interaction zone is controlled with a pyrometer with an operating range from 250 to 1300 °C and a response time of 15 µs. A spectral filter in the optical system of the pyrometer prevents effects from the reflected and scattered laser radiation. An oscilloscope is used to display the thermal cycles and to provide an interface to a PC.

For the thermal fatigue damage simulation four different pulse energies are chosen in order to achieve maximum surface temperatures of about 575, 600, 625 and 650 °C.

3 RESULTS

3.1. FEM analysis

FEM calculations were performed for (1) supporting the experimentation and for (2) analysing the thermo-mechanical loading situation of the irradiated specimen.

The choice of the testing parameters (laser power, interaction time, total cycle time) was based on FEM simulations. Furthermore, a comparison of the experimental and the computational results indicate proper experimentation, e.g. for the heat transfer from the disk shaped specimen to the temperature controlled mounting system. Thermo-physical (specific heat, thermal conductivity, Young's modulus) and thermo-mechanical (thermal expansion, temperature and strain rate dependent stress-strain curves) data of the DIN X 38 CrMoV 5 1 were determined in the temperature range from room temperature up to 650 °C in order to perform the FEM simulations.

Results of the FEM simulation of the temperature cycles are compared in Table 3 with pyrometrically measured temperatures. The results indicate an excellent accordance between measured and calculated surface temperatures for various absorbed pulse energies. The absorbed laser energy was estimated from the laser pulse energy assuming an absorption of 37%. The interaction time was 0,25 s and the total cycle time was 1 s.

Table 3 Comparison of calculated and measured surface temperatures

Absorbed pulse energy	Maximum surface temperature T_{max}		Surface temperature difference ΔT	
	Measured	Calculated	Measured	Calculated
49 J	575 °C	577 °C	304 °C	313 °C
52 J	600 °C	599 °C	322 °C	330 °C
56 J	625 °C	626 °C	338 °C	352 °C
59 J	650 °C	652 °C	366 °C	373 °C

For the chosen testing geometry a minimum number of cycles has to be considered to get stable results for the temperature cycles. Fig. 2 shows the development of the surface temperature within the first cycles indicating that the maximum temperature stabilises after about ten cycles.

The total strain ε_{ik} at each point of a heated body comprises of two components. In an elastic body the total strain can be described by Equation 1 [4,5]. $\alpha \cdot \Delta T$ is the uniform thermal expansion, the second part comprises the strains (stresses) required

to restrain the distortions of neighbouring elements to maintain the continuity of the body. If the stresses exceed the yield stress of the material, plastic strains occur too.

$$\varepsilon_{ik} = \frac{1}{2 \cdot G} \cdot \left[\sigma_{ik} - \frac{\nu}{1+\nu} \cdot \left(\sigma_{xx} + \sigma_{yy} + \sigma_{zz} \right) \cdot \delta_{ik} \right] + \alpha \cdot \Delta T \cdot \delta_{ik} \qquad (1)$$

$$\delta_{ik} = 0 \quad \text{for} \quad i \neq k$$

$$\delta_{ik} = 1 \quad \text{for} \quad i = k \qquad (i,k = x,y,z)$$

ε_{ik}... Total strain — G... Shear modulus — α... Thermal expansion coefficient

σ... Stress — ν... Poisson's ration — ΔT... Temperature difference

δ_{ik}... Factor

The FEM calculations were performed to estimate the strains and stresses for conditions which result in maximum surface temperatures of 577, 599, 626 and 652 °C. Figure 3 shows that the resulting equivalent thermally induced stresses increase from 428 to 502 MPa on raising the maximum surface temperature from 577 to 652 °C. The stress maximum occurrence corresponds to the time when the temperature maximum is reached. The stresses are compressive in the plane of the specimen surface, the stress normal to the surface is zero.

Figure 4 shows the strain components according to Equation 1 as a function of the maximum surface temperature. The thermal strain ε_{th} increases from about 0.47 to 0.59 % on increasing the maximum temperature from 577 to 652°C whereas the total strain ε_t increases from 0.29 to 0.32 %, the resulting elastic and plastic strains $\varepsilon_{e,p}$ increase from 0.19 to 0.24 %. Plastic straining even occurs in case of a maximum temperature of 575 °C. It can be also concluded from Figure 4 that the sum of the elastic and plastic strains are only about 41 % of the thermal strain.

Figure 5 shows the temporal evolution of the various strains (thermal strain ε_{th}, elastic and plastic strain $\varepsilon_{e,p}$ and total strain ε_t) for a temperature cycle with a maximum temperature of 650 °C. The results in Figure 5 are taken after the tenth cycle. The elastic and plastic strain $\varepsilon_{e,p}$ is compressive during the thermal loading and thus negative.

Figure 6 shows the radial stress – radial strain curve for a maximum surface temperature of 650 °C. Significant plastic deformation occurs in the first cycle, causing a stress reduction. The hysteresis loop shown in Figure 6 is more or less caused by the temperature variation in the surface near regions. Plastic strains are accumulated during thermal cycling, which causes a successive change of the maximum and minimum stresses (varying R-value). In the following considerations the strain range was taken to describe the loading situation during thermal cycling.

⊥

□

3.2 Experimental results

To characterise the thermal fatigue response of the tool steel DIN X 38 CrMoV 5 1 the surface of the irradiated specimens was inspected after defined numbers of cycles.

The surface was inspected in a scanning electron microscope in order to determine changes in the surface morphology and to determine the number of cycles to initiate fatigue cracks.

Additional Vickers hardness measurements with a load of 10N were carried out. The hardness measurements were performed at room temperature after applying the numbers of thermal cycles outlined above. The results of these hardness tests are shown in Figure 7. A hardness loss occurs at all investigated maximum temperature levels and the hardness loss increases significantly with increasing maximum temperature. This hardness loss is caused by cyclic softening due to plastic deformation.

Surface investigations by means of SEM reveal morphological changes of the polished surfaces. Figure 8 shows the sample surface after 3000 cycles at a maximum temperature of 650°C. Thermal cycling makes the martensitic structure visible. The observed surface roughness is a result of the inhomogeneous plastic deformation in the differently oriented martensite crystals. It can be further seen from Figure 8 that martensite and prior austenite grain boundaries are acting as preferred crack nucleation sites.

The crack nuclei are growing with increasing numbers of cycles laterally and into the depth. If the cracks reach a critical size they start building a network, Figure 9. The number of cycles to form a crack network was determined for the various maximum temperatures and the results are summarised in Figure 10. The strain range in Figure 10 was calculated by FEM as outlined above. The results indicate the strong influence of the maximum surface temperature on the number of cycles to form a network of cracks.

4 CONCLUSIONS

Thermal fatigue is an important damage mechanism significantly affecting the lifetime of tools, e.g. dies, which are subjected to cyclic thermal loads. A special thermal fatigue testing facility was designed and built-up to perform thermal fatigue tests in a very flexible and comfortable way. It was applied to characterise the thermal fatigue behaviour of hot working tool steels in very short time and under well-defined testing conditions.

FEM simulations were employed to support experimentation and to estimate the thermo-mechanical loading situation. Good accordance was found between the calculated and the experimentally determined surface temperatures. The FEM

⊥

□

calculations give also a good indication for the appearance of plastic deformations in the heated surface.

ACKNOWLEDGEMENT

Financial support by the TiG (Technologie und Impulse GmbH), the County of Styria (Land Steiermark), the SFG (Steiermärkische Forschungs- und Entwicklungsförderungsges.m.b.H) and the Municipality of Leoben within the framework of the Competence Center Programme Kplus is highly appreciated.

REFERENCES

(1) Zhang, Z., Delanges, D., and Bernhart, G., Stress-Strain Behaviour of Tool Steels under Thermomechanical Loading: Experiments and Modelling, *Proceedings of the 5th International Conference on Tolling*. Edited by Jeglitsch F., Ebner R., Leitner H., Leoben, Austria, 1999.

(2) Machlin, E., *Dislocation Theory of the Fatigue of Metals*, National Advisory Committee for Aeronautics, U.S.A., Report No. 1489, 1948.

(3) Pokora, E., Seif, H., Klein, F., *Thermisch bedingte Spannungen in Druckgießformen*, 12.Aalener Gießereisymposium, Germany, 1991.

(4) Melan, E., and Parkus, H., *Wärmespannungen*, Springer-Verlag, Wien, Austria, 1953.

(5) Boley, B., *Theory of Thermal Stresses*, Columbia Institute of Flight Structures, U.S.A., Krieger, 1985.

⊥

□

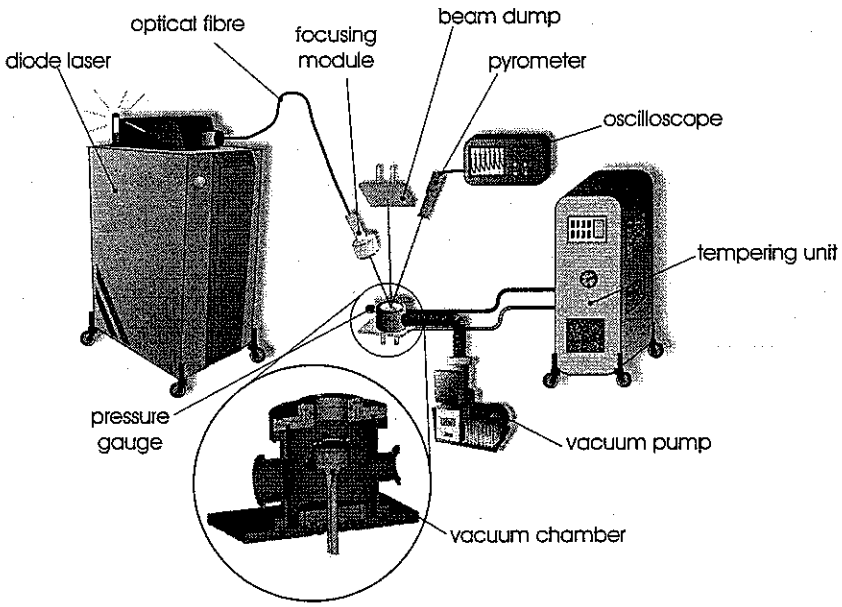

FIGURE 1 Thermal fatigue-testing rig

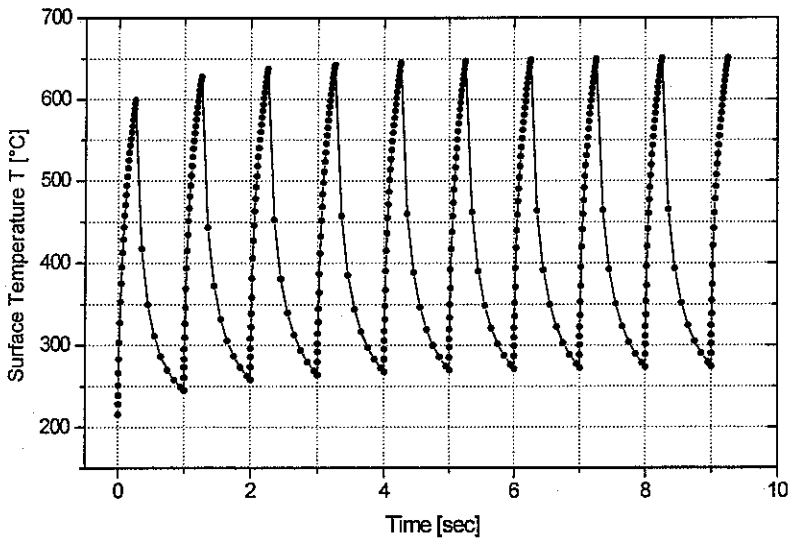

FIGURE 2 Calculated surface temperature cycles for pulse energy of 59 J

⊥

□

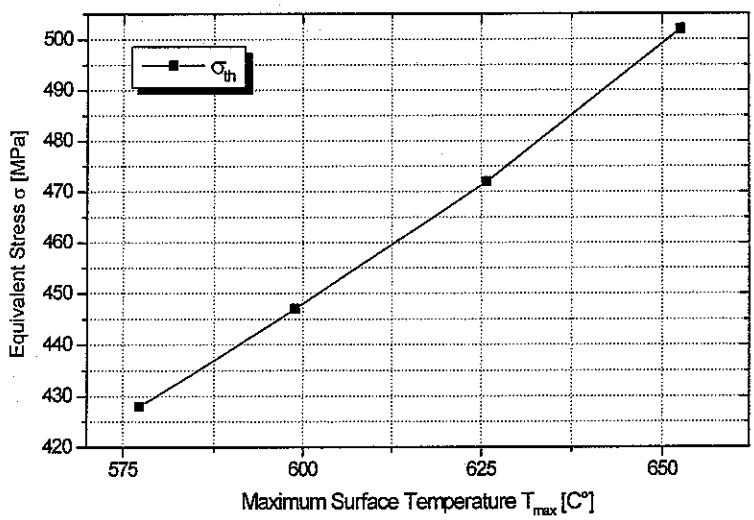

FIGURE 3 Calculated equivalent stress range for different maximum surface temperatures after 10 cycles

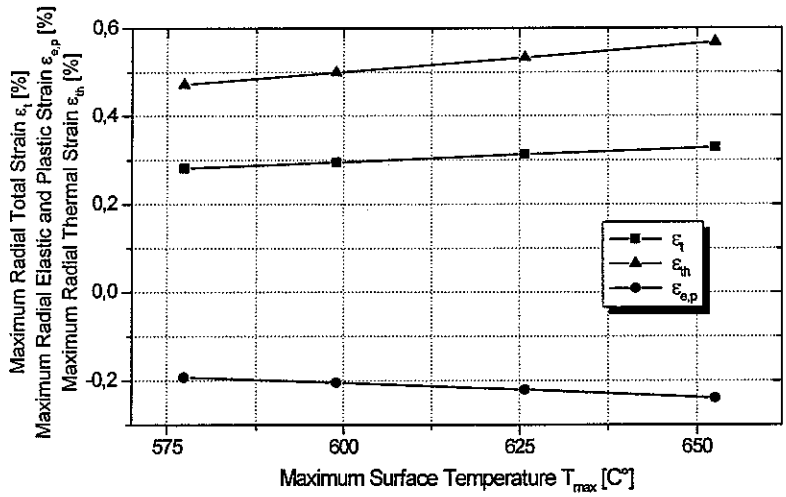

FIGURE 4 Calculated maximum radial strains for different maximum surface temperatures after 10 cycles

⊥

□

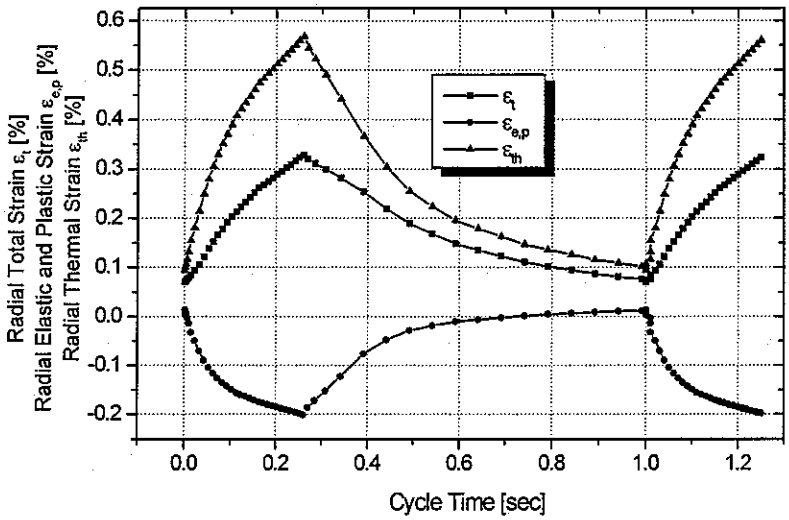

FIGURE 5 Calculated radial strains for the maximum surface temperatures of 650 °C during the tenth cycle

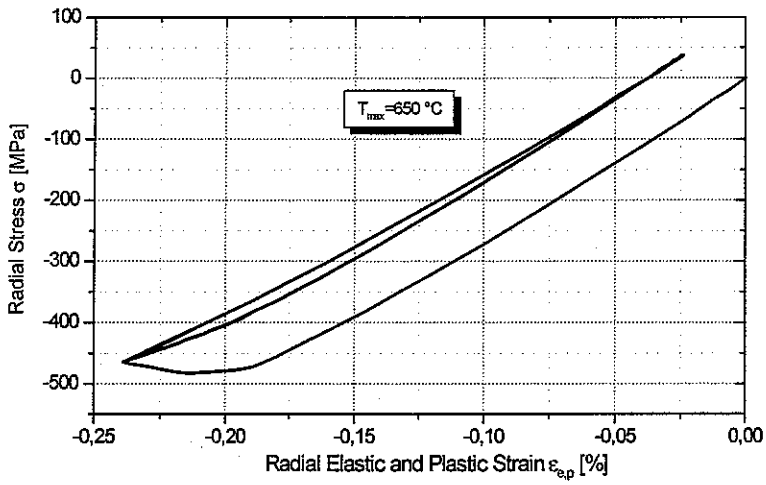

FIGURE 6 Calculated radial stress-strain cycle for maximum surface temperature of 650 °C

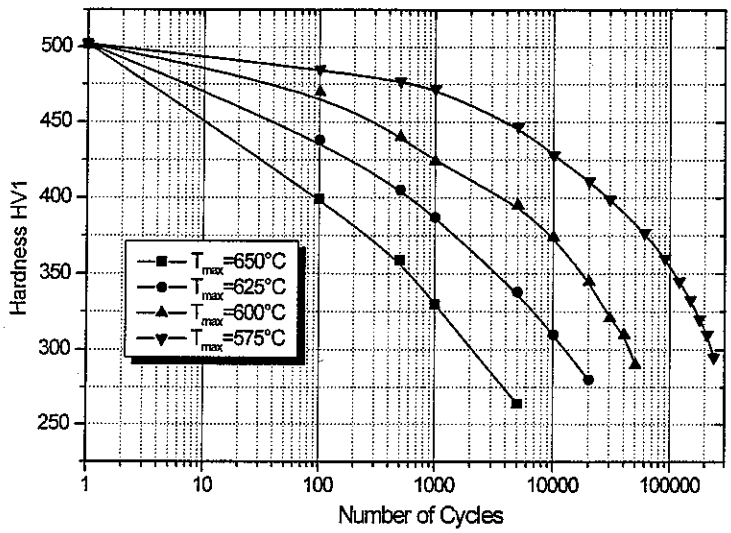

200°C underground temps

FIGURE 7 Hardness decrease versus number of cycles for different maximum surface temperatures

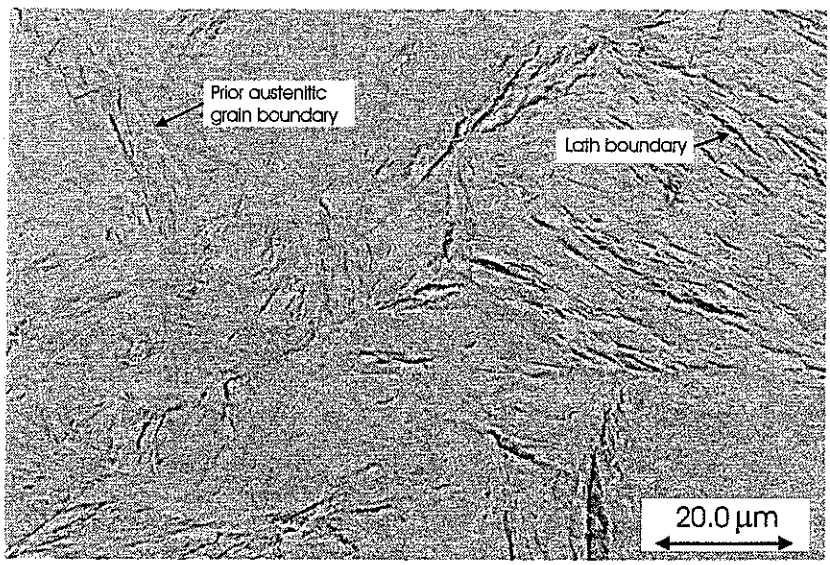

FIGURE 8 Scanning electron micrograph after thermal cycling (T_{max}=650 °C, 3000 cycles)

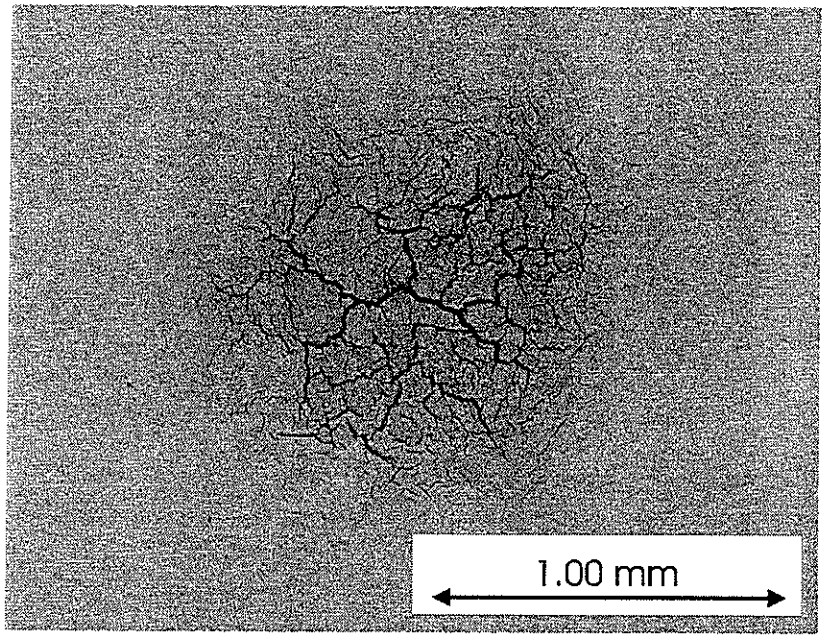

FIGURE 9 Scanning electron micrograph of a crack network (T_{max}=625°C, 45000 cycles)

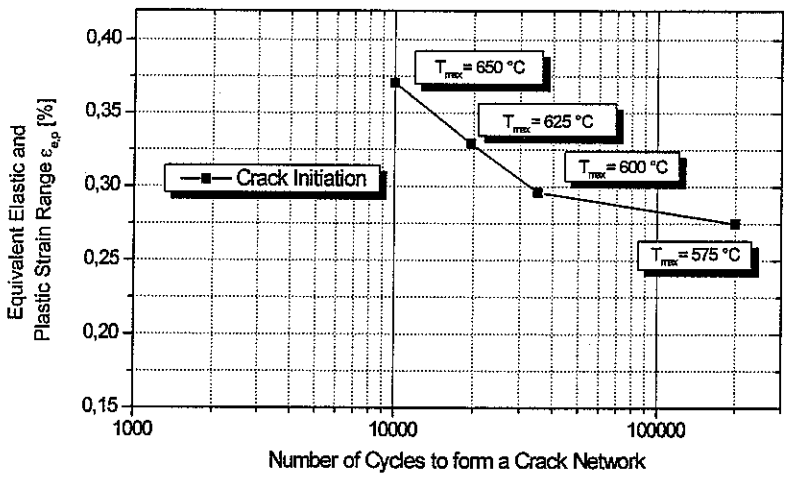

FIGURE 10 Crack initiations versus number of cycles at different maximum surface temperatures

⊥

□